

# Upper limit of the total cross section for the $pn \rightarrow pnn'$ reaction

J. Klaja,<sup>1,2,\*</sup> P. Moskal,<sup>1,2,\*</sup> S. D. Bass,<sup>3</sup> E. Czerwiński,<sup>1,2</sup> R. Czyżykiewicz,<sup>1</sup> D. Gil,<sup>1</sup> D. Grzonka,<sup>2</sup> T. Johansson,<sup>4</sup> B. Kamys,<sup>1</sup> A. Khoukaz,<sup>5</sup> P. Klaja,<sup>2,6</sup> W. Krzemień,<sup>1,2</sup> W. Oelert,<sup>2</sup> B. Rejdych,<sup>1</sup> J. Ritman,<sup>2</sup> T. Sefzick,<sup>2</sup> M. Siemaszko,<sup>7</sup> M. Silarski,<sup>1</sup> J. Smyrski,<sup>1</sup> A. Täschner,<sup>5</sup> M. Wolke,<sup>2,4</sup> P. Wüstner,<sup>2</sup> J. Zdebik,<sup>1</sup> M. Zieliński,<sup>1</sup> and W. Zipper<sup>7</sup>

<sup>1</sup>*Institute of Physics, Jagiellonian University, PL-30-059 Cracow, Poland*

<sup>2</sup>*Institute for Nuclear Physics and Jülich Center for Hadron Physics, Research Center Jülich, D-52425 Jülich, Germany*

<sup>3</sup>*Institute for Theoretical Physics, University of Innsbruck, Austria*

<sup>4</sup>*Department of Physics and Astronomy, Uppsala University, Sweden*

<sup>5</sup>*IKP, Westfälische Wilhelms-Universität, D-48149 Münster, Germany*

<sup>6</sup>*Physikalisches Institut, Universität Erlangen-Nürnberg, D-91058 Erlangen, Germany*

<sup>7</sup>*Institute of Physics, University of Silesia, PL-40-007 Katowice, Poland*

(Dated: January 17, 2014)

The upper limit of the total cross section for the  $pn \rightarrow pnn'$  reaction has been determined near the kinematical threshold in the excess energy range from 0 to 24 MeV. The measurement was performed using the COSY-11 detector setup, a deuteron cluster target, and the proton beam of COSY with a momentum of 3.35 GeV/c. The energy dependence of the upper limit of the cross section was extracted exploiting the Fermi momenta of nucleons inside the deuteron. Comparison of the determined upper limit of the ratio  $R_{\eta'} = \sigma(pn \rightarrow pnn')/\sigma(pp \rightarrow pp\eta')$  with the corresponding ratio for  $\eta$ -meson production does not favor the dominance of the  $N^*(1535)$  resonance in the production process of the  $\eta'$  meson and suggests nonidentical production mechanisms for  $\eta$  and  $\eta'$  mesons.

PACS numbers: 3.60.Le, 13.85.Lg, 14.20.Dh, 14.40.-n

Keywords: Near threshold  $\eta'$  production

## I. INTRODUCTION

Studies of  $\eta$  and  $\eta'$  mesons and their interactions with nucleons provide an interesting window on axial U(1) dynamics. The flavor-singlet  $J^P = 1^+$  channel is characterized by a large Okubo-Zweig-Iizuka (OZI) violation: the masses of the  $\eta$  and  $\eta'$  mesons are 300–400 MeV larger than the values they would have if these mesons were pure would-be Goldstone bosons associated with spontaneously broken chiral symmetry [1, 2].

One needs extra mass in the singlet channel associated with nonperturbative topological gluon configurations and the QCD axial anomaly [3]. The strange quark mass induces considerable  $\eta$ - $\eta'$  mixing. For the physical  $\eta$ - $\eta'$  mixing angle  $-18$  degrees, the singlet component in the  $\eta$  has the potential to induce a factor of 2 increase in the  $\eta$ -nucleon scattering length  $a_{\eta N}$  relative to the value one would expect if the  $\eta$  were a pure octet state [4]. The flavor-singlet Goldberger-Treiman relation [5] relates  $\eta'$ -nucleon coupling to the small flavor-singlet axial charge measured in the proton spin puzzle [6].

The properties of  $\eta$  and  $\eta'$  mesons should manifest themselves in production and decay processes and in their interaction with nuclear matter. These processes are being studied in experiments from threshold [7] through high-energy collisions where anomalously high branching

ratios have been observed for  $D_s$  and  $B$ -meson decays to an  $\eta'$  plus additional hadrons [8, 9].

At the hadronic level, it is expected that the  $\eta'$  meson can be produced through the exchange and rescattering of mesons, through the excitation of an intermediate baryonic resonance or via the fusion of virtual mesons [10–14]. So far the  $pn \rightarrow pnn'$  process has been studied quantitatively only within (i) an effective Lagrangian approach, assuming that the  $S_{11}(1535)$  resonance is dominant [13] and (ii) within a covariant effective meson-nucleon theory including meson and nucleon currents with the nucleon resonances  $S_{11}(1650)$ ,  $P_{11}(1710)$  and  $P_{13}(1720)$  [12]. However, for  $\eta'$  production there is an additional potential contribution where glue is excited in the “short distance” ( $\sim 0.2$ -fm) interaction region of the proton-nucleon collision and then evolves to become an  $\eta'$  in the final state. This gluonic contribution to the cross section for  $pp \rightarrow pp\eta'$ , proposed by Bass [14], is beyond the contributions associated with meson exchange models. There is no reason, a priori, to expect this OZI violating process to be small. Because glue is flavor-blind it contributes with the same strength in both the  $pp \rightarrow pp\eta'$  and the  $pn \rightarrow pnn'$  reactions.

It is not possible to establish the relative contributions of possible reaction mechanisms responsible for  $\eta'$ -meson production based only on the presently available cross sections for the  $pp \rightarrow pp\eta'$  reaction [15]. Therefore, one has to investigate  $\eta'$  production as a function of spin and isospin degrees of freedom. Such studies were conducted in the case of the  $\eta$  meson [16–18]. The ratio

\*Electronic address: p.moskal@fz-juelich.de

$R_\eta = \sigma(pn \rightarrow pn\eta)/\sigma(pp \rightarrow pp\eta)$  has been measured for quasifree  $\eta$  production from a deuteron target up to 109 MeV above threshold [16, 17]. One finds that  $R_\eta$  is approximately energy independent with a value of  $\sim 6.5$  in the energy range of 16 – 109 MeV signifying a strong isovector exchange contribution to the  $\eta$  production mechanism.

The ratio  $R_{\eta'}$  has not been measured to date, and the existing predictions differ drastically depending on the model. Cao and Lee [13] assumed, by analogy to the production of the  $\eta$  meson, that the production of the  $\eta'$  meson proceeds dominantly via the  $S_{11}(1535)$  resonance. As a consequence they predicted within an effective Lagrangian approach an  $R_{\eta'}$  value equal to the experimentally established  $R_\eta$  value. In contrast, Kaptari and Kämpfer [12] predicted a value of  $R_{\eta'}$  close to  $\sim 1.5$  in the kinematic range of the COSY-11 experiment with the dominant contribution coming from the meson conversion currents. In the extreme scenario of glue-induced production saturating the  $\eta'$  production cross section, the ratio  $R_{\eta'}$  would approach unity after correction for the final-state interaction between the two outgoing nucleons.

The SU(3) wave functions of the  $\eta$  and  $\eta'$  mesons differ due to iso-singlet gluonic and strangeness degrees of freedom. Hence, it is reasonable that singlet currents will play a greater role in  $\eta'$  than in  $\eta$  production. Proton-proton data are available from COSY and SATURNE [15]. To investigate the production mechanism it is important to provide an empirical base with spin and isospin dependence of the cross sections. In this article we present first results on the measurement of the  $pn \rightarrow pn\eta'$  reaction.

## II. EXPERIMENTAL TECHNIQUE

The COSY-11 detector system [19] is schematically depicted in Fig.1. A quasifree proton-neutron reaction was induced by a proton beam [20] with a momentum of 3.35 GeV/c impinging on a deuteron cluster target [21]. A detailed description of the functioning of the detectors and of the experimental technique is given in a recent COSY-11 article devoted to measurement of the  $pn \rightarrow pn\eta$  reaction [17] and in Ref. [22]. Therefore, we describe it only briefly here.

The experiment is based on the registration of all outgoing nucleons from the  $pd \rightarrow ppnX$  reaction. The proton moving forward is measured in two drift chambers and scintillator detectors and the neutron is registered in the neutral particle detector. The proton moving backward is measured with a dedicated silicon-pad detector [23]. In the data analysis the backward proton from the deuteron is considered as a spectator that does not interact with the bombarding proton, but escapes untouched and hits the detector carrying the Fermi momentum possessed at the time of the reaction. The total energy available for the quasifree proton-neutron reac-

tion is calculated for each event based on the momentum vectors of the spectator and beam protons under the assumption that the spectator proton is on its mass shell at the moment of the collision. The absolute momentum of the neutron is determined from the time of flight between the target and the neutron detector and its direction is derived from the hit position defined as the center of the detection module whose signal was produced as the first one. The veto detector installed in front of the neutral

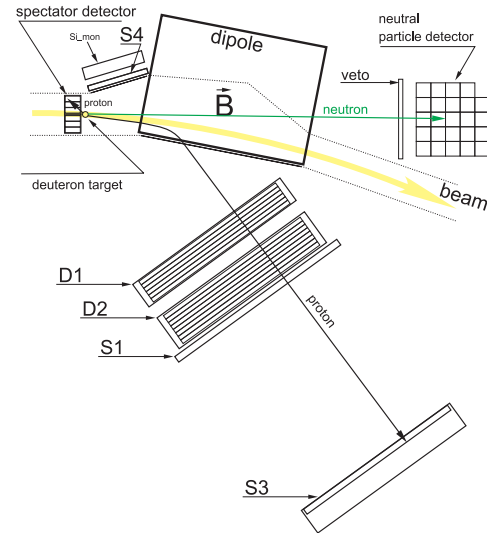


FIG. 1: Scheme of the COSY-11 detector system with superimposed tracks from the  $pd \rightarrow p_{spec}(pn\eta')$  reaction. Protons are registered in two drift chambers D1 and D2 and in the scintillator hodoscopes S1 and S3. The S1 detector is built of 16 vertically arranged modules, whereas the S3 hodoscope is a nonsegmented scintillator wall viewed by a matrix of 217 photomultipliers. An array of silicon pad detectors (spectator detector) is used for registration of spectator protons. Neutrons are registered in the neutral particle detector consisting of 24 independent detection units. To distinguish neutrons from charged particles a veto detector is used. Elastically scattered protons are measured in the scintillator detector S4 and the position-sensitive silicon detector  $Si_{mon}$ . The sizes of the detectors and their relative distances are not to scale.

particle detector discriminates signals originating from charged particles, whereas the  $\gamma$  quanta are discerned by means of the time of flight measured between the target and the neutral particle detector where the time of the reaction in the target is reconstructed based on the trajectory and velocity of the forward scattered protons detected in drift chambers and S1 and S3 scintillators. Figure 2 presents the momentum distribution of protons considered as spectators (crosses) compared with simulations taking into account a Fermi motion of nucleons inside the deuteron (solid line). In the analysis of the  $pn \rightarrow pn\eta'$  reaction spectator protons with momenta ranging from about 35 to about 115 MeV/c were taken into account. The lower limit is caused by the noise level of the silicon pad detectors. The *spectator noise cut* was determined for each pad of the detector separately, us-

ing the spectra of energy loss triggered by a pulser with a frequency of 1 Hz in addition to other experimental triggers. Protons with a momentum larger than about 115 MeV/c were not taken into account because we used the second layer of the double-layer spectator detector as a veto to reduce the background from charged pions. The shapes of the simulated and experimental spectra shown in Fig. 2 agree quite well, and the small difference will be taken for the estimation of the systematical uncertainties of the final results caused by the assumption of a Fermi momentum distribution of nucleons inside the deuteron.

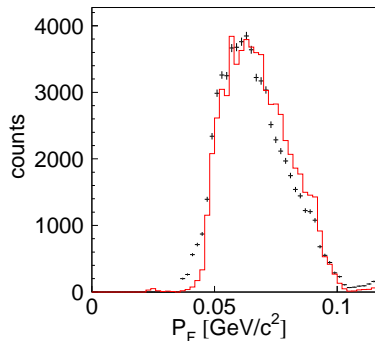


FIG. 2: Momentum distribution of the spectator proton as reconstructed in the experiment (crosses) in comparison with simulations taking into account the Fermi momentum distribution of nucleons inside the deuteron according to the Paris potential [24] (solid histogram). Simulated events were analyzed in the same way as the experimental data.

The accuracy of the excess energy determination was estimated based on Monte Carlo simulations. For this purpose we simulated  $10^9$  events of the  $pn \rightarrow pn\eta'$  reaction taking into account the Fermi motion of the nucleons inside the deuteron, the size of the target [21], the spread of the beam momentum and the horizontal and vertical beam size [25]. Simulated data were analyzed in the same way as the experimental data, taking into consideration the energy and time resolution of the detectors, resulting in an excess energy resolution of  $\sigma(Q) = 4.2$  MeV. It is worth stressing that using this method for the  $pn \rightarrow pn\eta'$  reaction the standard deviation of the excess energy was derived to be  $\sigma(Q) = 2.2$  MeV [17], which is comparable to the  $\sigma(Q) = 1.8$  MeV obtained under similar conditions at the PROMICE/WASA setup [23].

For further analysis the collected data were grouped according to the excess energy. The available range of excess energy  $Q$  above the  $\eta'$ -meson production threshold has been divided into three 8 MeV-wide intervals. The choice of the width of the interval is a compromise between statistics and resolution and reflects the accuracy (FWHM) of the determination of the excess energy. In Figs 3(a), 3(c), 3(e) the experimental mass distributions determined for the excess energy ranges [0, 8], [8, 16]

and [16, 24] MeV are shown by solid lines. For all distributions we observe an increase in counting rate toward the kinematical limit. The shape is mostly caused by the detector acceptance. A signal from the  $\eta'$ -meson production is expected on top of the continuous multipion mass distribution at the position corresponding to the  $\eta'$  mass ( $0.95778$  GeV/ $c^2$ ) [26], which is denoted by the arrow in Fig. 3. However, no enhancement around this region is seen.

To extract a signal the histograms corresponding to positive  $Q$  intervals were compared to the background established from the data below the threshold. For each distribution of the missing mass spectra at  $Q \geq 0$ , a corresponding background spectrum was constructed from events with  $Q$  belonging to the range  $[-30, -10]$  MeV by applying the method described in detail in a dedicated article [27]. This method was already applied successfully to the analysis of the  $pn \rightarrow pn\eta$  reaction [17]. As a cross-check, to gain more confidence in the applied procedure we constructed alternative background distributions taking events from the  $Q$  range from -20 to 0 MeV. The result of this investigation has shown a consistency of both background shapes of the order of 1%. Next, for each distribution for  $Q \geq 0$  the corresponding background spectrum was normalized for mass values smaller than  $0.25$  GeV/ $c^2$  where no events from the  $\eta'$  meson are expected. In this region events correspond to one-pion production, for which the total cross section remains nearly constant in the range of the excess energy shown, because for a single-pion production the excess energy is high above the threshold [27]. The dashed lines in Fig. 3 depict the background spectrum, shifted to the kinematical limit and normalized accordingly. The normalization in the missing mass range significantly below the mass of the  $\eta'$  meson (in the range from  $0.75$  to  $0.85$  GeV/ $c^2$ ) leads to the same result.

Figures 3 (b), 3(d), 3(f) show distributions of the missing mass for the  $pn \rightarrow pn\eta'$  reaction as determined after subtraction of the background. Because of the low statistics and very low signal-to-background ratio the signal from  $\eta'$ -meson created in the proton-neutron collision is statistically insignificant. Therefore, we can only estimate the upper limit for the  $\eta'$  meson production in the  $pn \rightarrow pn\eta'$  reaction.

To estimate the systematic error of the number of  $pn \rightarrow pnX$  events, the change in the missing mass spectra was studied by varying different parameters describing the experimental conditions, discussed in the following analysis and simulation [22]. The change in the global time offset of the neutral particle detector by 1 standard deviation of its time resolution ( $\sigma_t^N = 0.4$  ns) resulted in a systematic error of the cross sections of 3%. A change in simulations of the time resolution of the neutron detector (0.4 ns) by  $\pm 0.2$  ns resulted in  $\pm 5\%$  changes in the cross section. The variation in the cut on the noises in the spectator detector within the limits of energy resolution results in a change of cross sections by  $\pm 7\%$ . In the simulation we also checked that varying the beam momentum

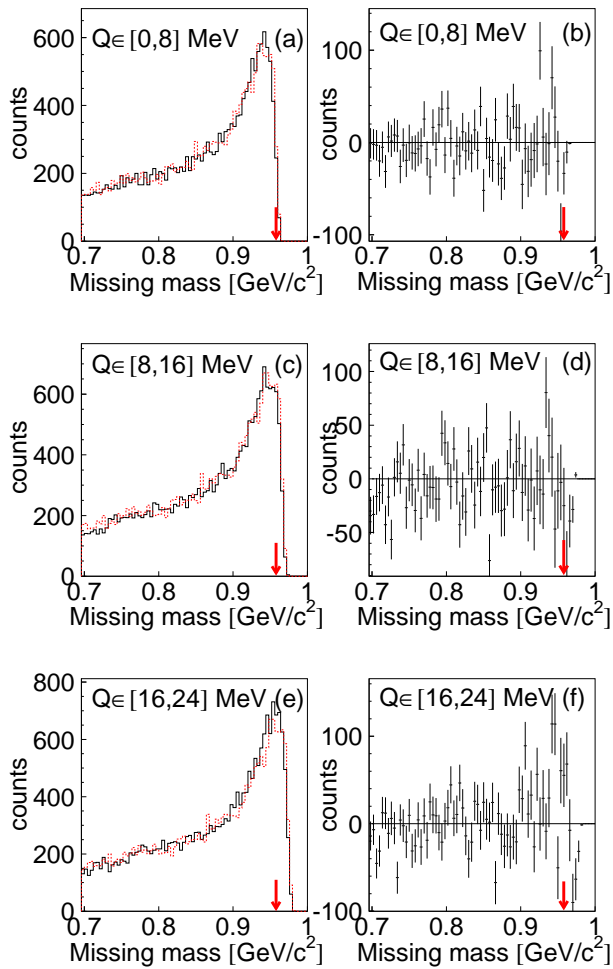


FIG. 3: (a, c, e) Experimental missing mass distributions of the  $pn \rightarrow pnX$  reaction (solid lines). Distributions were obtained for ranges of excess energy  $Q$  from 0 to 8 MeV (a), from 8 to 16 MeV (c) and from 16 to 24 MeV (e). Corresponding background spectra are shown as dashed lines. (b, d, f) Experimental missing mass distributions of the  $pn \rightarrow pn\eta'$  reaction for excess energy ranges from 0 to 8 MeV (b), from 8 to 16 MeV (d) and from 16 to 24 MeV (f) determined after background subtraction. Vertical bars indicate statistical errors. The arrow depicts the nominal value of the  $\eta'$  mass.

resolution arbitrarily by  $\pm 1$  MeV/c around its nominal value of 3.35 MeV/c resulted in changes in the cross section values by  $\pm 3\%$ . As discussed previously, and demonstrated in Ref. [27], the systematic error owing to the method used for the background subtraction is equal to 1%. The uncertainty owing to the model dependence calculation of the Fermi momentum distribution is equal to 2% [28] and was estimated as the difference in results determined using the Paris [24] versus the CD-Bonn [29] potentials. It is worth stressing that also a difference between the experimental Fermi momentum distribution and the predictions based on the Paris potential leads to a variation in the final result of about 2%. A displace-

ment of the spectator detector by 1 mm (the estimated accuracy of its position determination) changes the number of events by 5%. The error of the detection efficiency, predominantly caused by the uncertainty in the efficiency of the neutral particle detector [30], is determined to be no larger than 5% [17]. We also took into account the systematic error ( $\sigma L_{int} \approx 7\%$  [22]) originating from the luminosity determination. The nuclear “shadow effect” (estimated to about 4.5% [31]) was not taken into account because the reduction of the beam flux seen by the neutron, owing to the shielding by a spectator proton, is expected to be the same for the  $pn \rightarrow pn\eta'$  reaction and quasielastic scattering that was used for determination of the luminosity. Similarly we have neglected the effect owing to the reabsorption of the produced meson by the spectator proton, because even for the case of  $\eta$ -meson production this effect reduces the cross section by a factor of about 3% [32] and the proton- $\eta$  interaction is much stronger than the proton- $\eta'$  interaction [33]. Finally, the total systematic error of  $\sigma^{TOT}(Q)$  was estimated as the quadratic sum of the nine independent systematic errors discussed and is equal to  $\approx 14\%$ .

### III. RESULTS

The luminosity of  $L = 4.77 \text{ pb}^{-1} \pm 0.06 \text{ pb}^{-1}$  was established from the number of quasifree proton-proton scattering events applying the method described in the dedicated article [34]. The acceptance of the detector setup and efficiency was determined based on Monte Carlo studies. The signal from the  $\eta'$  meson in the determined missing mass spectra is statistically insignificant. Therefore only the upper limit of the total cross section for the quasifree  $pn \rightarrow pn\eta'$  reaction was extracted. The number of  $\eta'$  mesons can be calculated as the difference between the number of events ( $N^{SIG}$ ) in the peak for the signal (solid line in Fig. 3) and the number of events ( $N^{BACK}$ ) in the background of the peak (dashed line in Fig. 3):

$$N^{\eta'} = (N^{SIG} - N^{BACK}) \pm \sqrt{N^{SIG} + N^{BACK}}. \quad (1)$$

The range for the integration was chosen based on the simulation of the missing mass distributions [22]. Assuming that no  $\eta'$  mesons are observed ( $N^{\eta'} = 0$ ) in the experiment, the value of  $1.2815 \times \sqrt{N^{SIG} + N^{BACK}}$  gives the upper limit of the total cross section for the  $pn \rightarrow pn\eta'$  reaction at a 90% confidence level. The result is shown in Fig. 4 and in Table I.

The horizontal bars in Fig. 4 represent the intervals of the excess energy for which the upper limit of the total cross section was calculated.

The total cross section for the  $pp \rightarrow pp\eta'$  reaction was measured in previous experiments [15]. It reveals a strong excess energy dependence, especially very close to threshold. This dependence must be taken into account when comparing the results for the  $pn \rightarrow pn\eta'$

$Q$ (MeV)	Upper limit of $\sigma(pn \rightarrow pn\eta')$ at 90% CL (nb)	$\sigma(pp \rightarrow pp\eta')$ (nb)	Upper limit of $R_{\eta'}$ at 90% CL
[0, 8]	63	19.6	3.2
[8, 16]	197	68.7	2.9
[16, 24]	656	122.7	5.3

TABLE I: Excess energy range, upper limit of the total cross section for the  $pn \rightarrow pn\eta'$  reaction, mean value of the  $pp \rightarrow pp\eta'$  total cross section according to the parametrization given in Ref. [35], upper limit of the ratio  $R_{\eta'}$ , as a function of the excess energy. Energy intervals correspond to the binning applied.

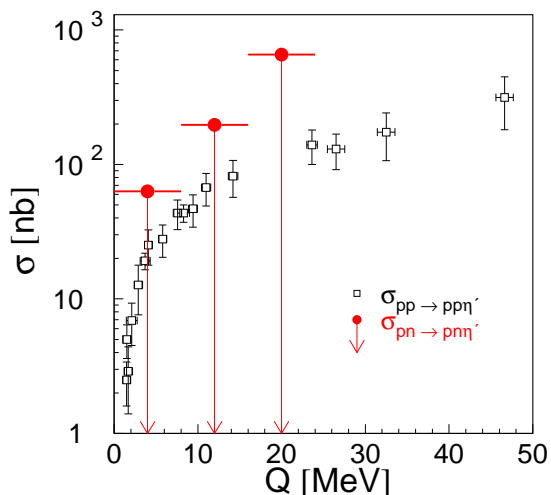


FIG. 4: Total cross sections for the  $pp \rightarrow pp\eta'$  reaction as a function of the excess energy (open squares). Upper limit for the total cross section for the  $pn \rightarrow pn\eta'$  reaction as a function of the excess energy (filled circles).

reaction that were established for 8-MeV excess energy intervals. Therefore, for a given interval of excess energy, we have determined the mean value of the total cross section for  $pp \rightarrow pp\eta'$  reaction using the parametrization of Fäldt and Wilkin [36, 37] fitted to the experimental data [35]. Figure 5 presents the upper limit of the ratio  $R_{\eta'} = \sigma(pn \rightarrow pn\eta')/\sigma(pp \rightarrow pp\eta')$  of the total cross section for the  $pn \rightarrow pn\eta'$  and  $pp \rightarrow pp\eta'$  reactions as a function of the excess energy (arrows). The corresponding values are listed in Table I. The corresponding ratios for the  $\eta$  meson are also shown as open squares in Fig 5. For the  $\eta$  meson, the value of  $R_{\eta}$  is  $\approx 6.5$  at excess energies larger than  $\sim 16$  MeV [16], which suggests the dominance of isovector-meson exchange in the production mechanism. The decrease in  $R_{\eta}$  close to the threshold [17] may be explained by the different energy dependence of the proton-proton and proton-neutron final-

state interactions [38].

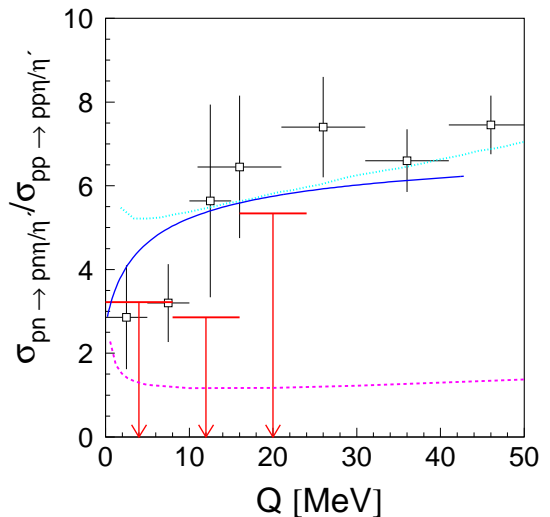


FIG. 5: Upper limit of the ratio ( $R_{\eta'}$ ) of the total cross sections for the  $pn \rightarrow pn\eta'$  and  $pp \rightarrow pp\eta'$  reactions (arrows) in comparison with the ratio ( $R_{\eta}$ ) determined for the  $\eta$  meson [16, 17] (open squares). The superimposed solid line indicates the result of a fit to the  $R_{\eta}$  data taking into account the final-state interaction of nucleons [17]. The dotted line presents the result of calculations performed under assumption of dominance of the  $S_{11}(1535)$  resonance in the production process [13], and the dashed line denotes the result obtained within a covariant effective meson-nucleon theory including meson and nucleon currents with nucleon resonances  $S_{11}(1650)$ ,  $P_{11}(1710)$  and  $P_{13}(1720)$  [12]

For the  $\eta'$  meson the upper limit of the ratio for the excess energy range [0, 8] MeV is nearly equal to values of the ratio obtained for the  $\eta$  meson, whereas for larger excess energy ranges, [8, 16] and [16, 24] MeV, the upper limits of the ratio are lower by about 1 standard deviation each. The dotted curve in Fig. 5 corresponds to the prediction for  $R_{\eta'}$  by Cao and Lee [13] and exceeds the observed limit, showing the importance of other exchange currents in the  $\eta'$  production. The prediction of Kaptari and Kämpfer [12] is well within the upper bound. A smaller  $R_{\eta'}$  than  $R_{\eta}$  is also consistent with a possible greater role for singlet currents in  $\eta'$  production than  $\eta$  production. If there are important new dynamics in the  $\eta'$  production process relative to  $\eta$  production, a key issue is the relative phase [39] of possible additional exchanges compared to the isovector currents that dominate  $\eta$  production. The observed limit thus constrains modeling of the production processes. To confirm these interesting observations and to go farther, new experimental investigations with improved statistics are required.

#### IV. SUMMARY

To determine the excitation function of the total cross section for the quasifree  $pn \rightarrow pn\eta'$  reaction near the kinematical threshold, we performed an experiment at the cooler synchrotron COSY at the Research Centre Jülich using the COSY-11 detector system. The quasifree  $pn \rightarrow pn\eta'$  reaction was induced by a proton beam with a momentum of 3.35 GeV/c on a deuteron target. All outgoing nucleons have been registered, whereas for  $\eta'$ -meson identification the missing mass technique was applied. The upper limit of the total cross section for the  $pn \rightarrow pn\eta'$  reaction in the excess energy range between 0 and 24 MeV has been determined. The total cross section for the  $pp \rightarrow pp\eta'$  reaction was measured in previous experiments at the same energy range. Combining these data, we have determined the upper limit of the ratio  $R_{\eta'} = \sigma(pn \rightarrow pn\eta')/\sigma(pp \rightarrow pp\eta')$ . The comparison of the  $R_{\eta'}$  ratio with the upper limits of  $R_{\eta'}$  established here suggests nonidentical production mechanisms for the  $\eta'$  and  $\eta$  mesons, which are dominated by a strong isovector

exchange contribution. To pin down the detailed reaction mechanism further theoretical as well as experimental investigations with better statistics are required.

#### Acknowledgments

We are grateful for useful comments of Burkhard Kämpfer, Piotr Salabura and Joanna Stepaniak. The work was partially supported by the European Community-Research Infrastructure Activity under the FP6 and FP7 programs (Hadron Physics, RII3-CT-2004-506078, PrimeNet No. 227431), by the Polish Ministry of Science and Higher Education under Grant Nos 3240/H03/2006/31, 1202/DFG/2007/03, and 0082/B/H03/2008/34, by the German Research Foundation (DFG), by the FFE grants from the Research Center Jülich, by the Austrian Science Fund, FWF, through grant P20436 and by the virtual institute "Spin and strong QCD" (VH-VP-231).

- 
- [1] S. D. Bass, Phys. Scripta **T 99**, 96 (2002).
  - [2] S. D. Bass, Acta Phys. Polon. **B Proc. Suppl. 2**, 11 (2009).
  - [3] G.M. Shore, hep-ph/9812354; Lect. Notes Phys. **737**, 235 (2008) [hep-ph/0701171]
  - [4] S. D. Bass and A. W. Thomas, Phys. Lett. **B634**, 368 (2006).
  - [5] G.M. Shore and G. Veneziano, Phys. Lett. **B244**, 75 (1990); T. Hatsuda, Nucl. Phys. **B329**, 376 (1990).
  - [6] S. D. Bass, Rev. Mod. Phys. **77**, 1257 (2005).
  - [7] P. Moskal, M. Wolke, A. Khoukaz, W. Oelert, Prog. Part. Nucl. Phys. **49**, 1 (2002); P. Moskal, Habilitation Dissertation No. 364 (Jagiellonian University Press, Cracow, 2004), arXiv:hep-ph/0408162.
  - [8] P. Ball, J. M. Frere and M. Tytgat, Phys. Lett. **B 365**, 367 (1996).
  - [9] H. Fritzsche, Phys. Lett. **B 415**, 83 (1997).
  - [10] K. Nakayama, H. F. Arellano, J. W. Durso, and J. Speth, Phys. Rev. **C 61**, 024001 (2000).
  - [11] K. Nakayama and H. Haberzettl, Phys. Rev. **C 69**, 065212 (2004).
  - [12] L. P. Kaptari, B. Kämpfer, Eur. Phys. J. **A 37**, 69 (2008); B. Kämpfer (private communication).
  - [13] X. Cao and X.-G. Lee, Phys. Rev. **C 78**, 035207 (2008); X. Cao (private communication).
  - [14] S. D. Bass, Phys. Lett. **B 463**, 286 (1999).
  - [15] P. Klaja *et al.*, Phys. Lett. **B 684**, 11 (2010); A. Khoukaz *et al.*, Eur. Phys. J. **A 20**, 345 (2004); P. Moskal *et al.*, Phys. Lett. **B 474**, 416 (2000); F. Balestra *et al.*, Phys. Lett. **B 491**, 29 (2000); P. Moskal *et al.*, Phys. Rev. Lett. **80**, 3202 (1998); F. Hibou *et al.*, Phys. Lett. **B 438**, 41 (1998).
  - [16] H. Calén *et al.*, Phys. Rev. **C 58**, 2667 (1998).
  - [17] P. Moskal *et al.*, Phys. Rev. **C 79**, 015208 (2009).
  - [18] R. Czyżykiewicz *et al.*, Phys. Rev. Lett. **98** 122003 (2007).
  - [19] S. Brauksiepe *et al.*, Nucl. Instr. & Meth. **A376**, 397 (1996).
  - [20] D. Prasuhn *et al.*, Nucl. Instr. & Meth. **A 441**, 167 (2000).
  - [21] H. Dombrowski *et al.*, Nucl. Instr. & Meth. **A 386**, 228 (1997).
  - [22] J. Klaja, Ph.D. thesis, Jagiellonian University, 2009, e-Print: arXiv:0909.4399.
  - [23] R. Bilger *et al.*, Nucl. Instr. & Meth. **A 457**, 64 (2001).
  - [24] M. Lacombe *et al.*, Phys. Lett. **B 101**, 139 (1981).
  - [25] P. Moskal *et al.*, Nucl. Instr. & Meth. **A 466**, 488 (2001).
  - [26] C. Amsler *et al.*, Phys. Lett. **B 667**, 1 (2008).
  - [27] P. Moskal *et al.*, J. Phys. **G 32**, 629 (2006).
  - [28] R. Czyżykiewicz, Diploma thesis, **Jül-4017**, Jagiellonian University, 2002.
  - [29] R. Machleidt *et al.*, Phys. Rev. **C 63**, 024001 (2001).
  - [30] J. Klaja *et al.*, Acta Phys. Polon. **B Proc. Suppl. 2**, 31 (2009).
  - [31] E. Chiavassa *et al.*, Phys. Lett. **B 322**, 270 (1994).
  - [32] E. Chiavassa *et al.*, Phys. Lett. **B 337**, 192 (1994).
  - [33] P. Moskal *et al.*, Phys. Lett. **B 482** (2000) 356.
  - [34] P. Moskal and R. Czyżykiewicz, AIP Conf. Proc. **950**, 118 (2007).
  - [35] P. Moskal *et al.*, Int. J. Mod. Phys. **A 22**, 305 (2007).
  - [36] G. Fäldt and C. Wilkin, Phys. Lett. **B 382**, 209 (1996).
  - [37] G. Fäldt and C. Wilkin, Phys. Rev. **C 56**, 2067 (1997).
  - [38] C. Wilkin (private communication).
  - [39] G. Fäldt and C. Wilkin, Phys. Scripta **64**, 427 (2001).